Colloids and Surfaces B: Biointerfaces 208 (2021) 112083

Contents lists available at ScienceDirect

Colloids and Surfaces B: Biointerfaces

journal homepage: www.elsevier.com/locate/colsurfb

Nano-engineering stable contact-based antimicrobials: Chemistry at the interface between nano-gold and bacteria

Marija Vukomanovic [a,b,*], Maria del Mar Cendra [a], Aida Baelo [a], Eduard Torrents [a,c,**]

[a] Bacterial Infections: Antimicrobial Therapies, Institute for Bioengineering of Catalonia (IBEC), The Institute of Science and Technology (BIST), Baldiri Reixac 15-21, 08028, Barcelona, Spain
[b] Advanced Materials Department, Jozef Stefan Institute, Jamova 39, 1000, Ljubljana, Slovenia
[c] Microbiology Section, Department of Genetics, Microbiology and Statistics, Faculty of Biology, University of Barcelona, 643 Diagonal Ave., 08028, Barcelona, Spain

ARTICLE INFO

Keywords:
Antibiotic-free technology
Contact-based antimicrobials
Functionalized gold
Charged amino acids
Enzyme-resistant antimicrobials

ABSTRACT

Contact-based antimicrobials, as antibiotic-free technologies that use non-specific interactions with bacterial cells to exert antimicrobial activity, are a prospective solution in fighting the global issue of bacterial resistance. A very simplified approach to their design considers the direct bonding of cationic guanidine-containing amino acids to the surface of nano-gold carriers. The structure enables antimicrobial activity due to a high density of cationic surface charges. This opens a set of novel questions that are important for their effective engineering, particularly regarding (i) chemistry and events that take place at the interface between NPs and cells, (ii) the direct influence of a charge (and its change) on interactions with bacterial and mammalian cells, and (iii) the stability of structures (and their antimicrobial activity) in the presence of enzymes, which are addressed in this paper. Because of the ability of amino acid-functionalized nano-gold to retain structural and functional activity, even after exposure to a range of physicochemical stimuli, they provide an excellent nanotechnological platform for designing highly effective contact-based antimicrobials and their applications.

1. Introduction

The progressive increase in antimicrobial multiresistant (AMR) bacteria, followed by a gradual decrease in antibiotic efficacy, challenges current research in designing innovative antimicrobial therapies [1–5]. Despite the existence of very potent antibiotics, innovative nanotechnology-based antibiotic drug-delivery systems and antimicrobial nanoparticles, bacterial infections are still serious health issues [6]. A branch of the state-of-the-art in developing more efficient antimicrobial strategies is focused on engineering antibiotic-free options. An example of such a technology is innovative contact-based antimicrobials [7,8]. They do not release any soluble biocide molecules or ions. Unlike antibiotics, contact-based antimicrobials do not work through specific receptor-protein interactions [8]. Instead, they use non-specific (i.e., electrostatic) interactions that physically disaggregate bacterial cells and hold a significantly lower risk of developing bacterial resistance mechanisms [8,9]. This non-specific mechanism should be targeted to bacteria and should be kept stable over environmental factors (such as enzymes and pH) to obtain maximal efficacy.

Mainly designed as functionalized polymers [6,10], contact-based antimicrobials usually contain a high density of charged functional groups (i.e., quaternary ammonium compounds, alkyl pyridiniums, or quaternary phosphonium). They use multiple charges to attach and interact with bacterial membranes, enabling their disassembly and mechanical perforation [6]. The main limitation of these systems is low chemical stability under physiological environments and pronounced susceptibility to enzymatic degradation, characterized by some antimicrobial peptides (AMPs) and polymers, which are good targets for potential inactivation mechanisms [6].

Bonding charged molecules to the surface of inorganic materials, such as nano-gold (AuNPs) [11–14], that are characterized by much higher stability in physiological environments [15,16], could be a good alternative. Membrane-targeting antimicrobial activity, based on net charge and amphiphilic nature, is a strategy used by AMPs [17–19]. In the case of site-specific bonding, the chemical functionalization of AuNPs with AMPs does not affect the biologically active conformation

* Corresponding author at: Advanced Materials Department, Jozef Stefan Institute, Jamova 39, 1000, Ljubljana, Slovenia.
** Corresponding author at: Bacterial Infections: Antimicrobial Therapies, Institute for Bioengineering of Catalonia (IBEC), The Institute of Science and Technology (BIST), Baldiri Reixac 15-21, 08028, Barcelona, Spain.
E-mail addresses: marija.vukomanovic@ijs.si (M. Vukomanovic), etorrents@ibecbarcelona.eu (E. Torrents).

https://doi.org/10.1016/j.colsurfb.2021.112083
Received 6 November 2020; Received in revised form 20 July 2021; Accepted 29 August 2021
Available online 31 August 2021

[13]. As recently shown, AuNP-bonded peptides can fold into helical structures that dock with and perturb the bacterial membrane, exerting antimicrobial activity. Moreover, bonding to AuNPs effectively protected AMPs from enzymatic (proteolytic) deactivation, resulting in longer life times and better antimicrobial activity [13].

Technologically significantly simplified and economically more affordable approaches to mimicking AMPs include the direct bonding of amino acids to the surface of AuNPs as a tool for designing contact-based antimicrobials [16,20,21]. The arginine amino acid, with a guanidinium group in the side chain, was bonded directly to hydrophobic AuNPs templated on hydrophilic apatite [16,20,21]. Guanidine groups are strong bases with a positive charge delocalized among three nitrogen atoms, which makes them predominantly charged at different pH values and protonated at neutral and physiological pH, with high thermal and base stability [8,22]. Interactions between guanidine and phosphate groups, which result in hydrogen bond ion pair formation, are stronger than interactions between linear amines and phosphates, which contributes to a stronger antimicrobial effect [8]. In addition, the toxicity of delocalized charge in guanidine groups to mammalian cells is lower than the toxicity of charge in linear amine heads [8].

Bonding amino acids to AuNPs enables antimicrobial activity as a result of the formed structure—a high density of charge at the surface is available for non-specific interactions with components in bacterial membranes. This opens a set of novel questions highly important for engineering effective contact-based technology:

(i) How the nature of functionalizing amino acids and their functional groups contribute to the resultant antimicrobial activity;
(ii) What events take place at the interface between these structures and cells (bacterial and mammalian); and
(iii) Whether there are changes in the stability (and efficacy) of these structures, particularly after exposure to physiological conditions, including the presence of proteolytic enzymes.

These questions are the main focus of the research presented in this manuscript in pursuit of understanding the basics of charged amino acid technology and tailoring the concepts to similar contact-based antimicrobials.

2. Materials and methods

2.1. Materials

Chloroauric acid (Sigma-Aldrich, Germany), L-arginine (Sigma-Aldrich, Germany), L-arginine-7-amido-4-methyl-coumarin (Sigma-Aldrich, Germany), dansyl-L-arginine (Sigma-Aldrich, Germany), aspartic acid (Sigma-Aldrich, Germany), serine (Sigma-Aldrich, Germany), alanine (Sigma-Aldrich, Germany), calcium nitrate pentahydrate (Sigma-Aldrich, Germany), ammonium dihydrogen phosphate (Sigma-Aldrich, Germany) and urea (Alfa Aesar, Germany).

2.2. Synthesis of nano-gold/apatite with an amino acid-functionalized surface

The synthesis was performed using chemical precipitation in an ultrasonic field [20,21] with apatite as a template made by sonochemical homogeneous precipitation [23]. Fifty millilitres of an aqueous solution of $HAuCl_4$ (0.8 mg/mL) and 50 ml of an amino acid solution (arginine, arginine-coumarin, arginine-dansyl, aspartic acid, alanine or serine) in water (0.4 mg/mL) were added to apatite dispersed in water (1.5 mg/mL) and sonicated (Ultrasonic Processor for High Volume Applications VCX 750, Newtown, Connecticut, USA) for the next 30 min. The obtained precipitates were centrifuged (15 min at 4000 rpm) and air dried. Details are provided in the Supplementary file.

2.3. Methods of physicochemical characterization

Morphological and structural analyses were performed by transmission electron microscopy (TEM) (JEOL JEM-2100). Optical properties were analysed using UV–vis spectrophotometry (UV–vis-NIR spectrophotometer Shimadzu UV-3600). Zeta potential measurements were performed using a Malvern Nanosizer. Fourier transformed infrared spectroscopy (FTIR) of powders (5 mg of sample diluted with 70 mg of KBr) was performed using a Perkin Elmer Spectrum 400 MIR spectrophotometer with the DRIFT technique.

2.4. Bacterial growth kinetics study

The influence of NPs on bacterial growth kinetics was studied using the Presto blue method [24]. Tests were performed in two gram-negative strains, *E. coli* MG1655 (ATCC 47076) and *P. aeruginosa* PAO1 (ATCC 15692), and one gram-positive strain, *S. aureus* Rosenbach (ATCC 12600). Details are provided in the Supplementary file.

2.5. Cytotoxicity testing

All experiments were performed in human lung epithelial A549 cells. A549 cells treated with NPs were incubated at 37 °C in a 5% CO_2 atmosphere. After 24 h, 20 µl of 10x Presto blueTM Cell Viability Reagent (Molecular Probes, Invitrogen, Thermo Fisher Scientific) was used to evaluate viability. Details are provided in the Supplementary file.

2.6. Fluorescence microscopy analysis

Bacterial viability was investigated using Live/Dead BacLight staining (Invitrogen, Thermo Fisher). For bacterial membrane integrity, staining was performed using FM 464 (Invitrogen, Thermo Fisher)/DAPI (Biotium, Fremont, CA). Mammalian cell morphology was evaluated using DAPI/WGA/EthD III (Biotium, Fremont, CA) staining. Details are provided in the Supplementary file. Samples were analysed using the Nikon ECLIPSE Ti-S/L100.

2.7. SEM and TEM bacteria analyses

Morphological and structural analyses of bacterial cells with and without NPs were performed using FEISEM (Nova NanoSEM) and TEM (JEOL JEM-2100). Details are provided in the Supplementary file.

2.8. Enzymatic digestion study

The digestion test was performed using proteinase K (PanReac AppliChem) and trypsin-EDTA with red phenol (Thermo Fisher). Degradation products were analysed using SDS-PAGE (10 % acrylamide) (Biorad) and visualized after Coomassie blue staining using the Image Quant LAS4000 mini. After digestion, NPs were recovered and tested for antimicrobial activity. Details are provided in the Supplementary file.

2.9. Statistics

Results are presented as mean value ± SD. Differences between groups were assessed by one way (Anova) using the Bonferroni post-hoc test with $p \leq 0.0001$ (assigned with ****) versus control for each nanoparticle functionalization.

3. Results and discussion

The formation of contact-based antimicrobials by the direct bonding of small charged molecules (such as charged amino acids) to the NP surface without the formation of macromolecules and excluding the presence of enzyme-cleavable bonds (such as peptides) could yield exceptional stability and resistance to proteolytic enzymes. Following

this concept, we modified the nature of amino acids functionalized on the surface of nano-gold (AuNPs) and investigated the contributions of all relevant functional groups to the structural and functional stability (as illustrated in Fig. 1).

3.1. The nature of amino acids affects the stability of functionalized AuNPs as contact-based antimicrobials

Amino acids with different polarities and charges were employed for AuNP functionalization, including cationic and polar arginine, anionic and polar aspartic acid, non-charged and non-polar alanine, and polar serine (Fig. 1). The goal was to determine how the nature of each amino acid (polarity and charge) affected the properties of functionalized AuNPs as contact-based antimicrobials. We were also interested in the role of functional groups in stability and antimicrobial activity. For that purpose, we functionalized the AuNPs with amino acids with specific groups selectively blocked. As illustrated in Fig. 1, in contrast to arginine with free carboxylic (COOH-) and amine (NH_2-) groups, arginine-

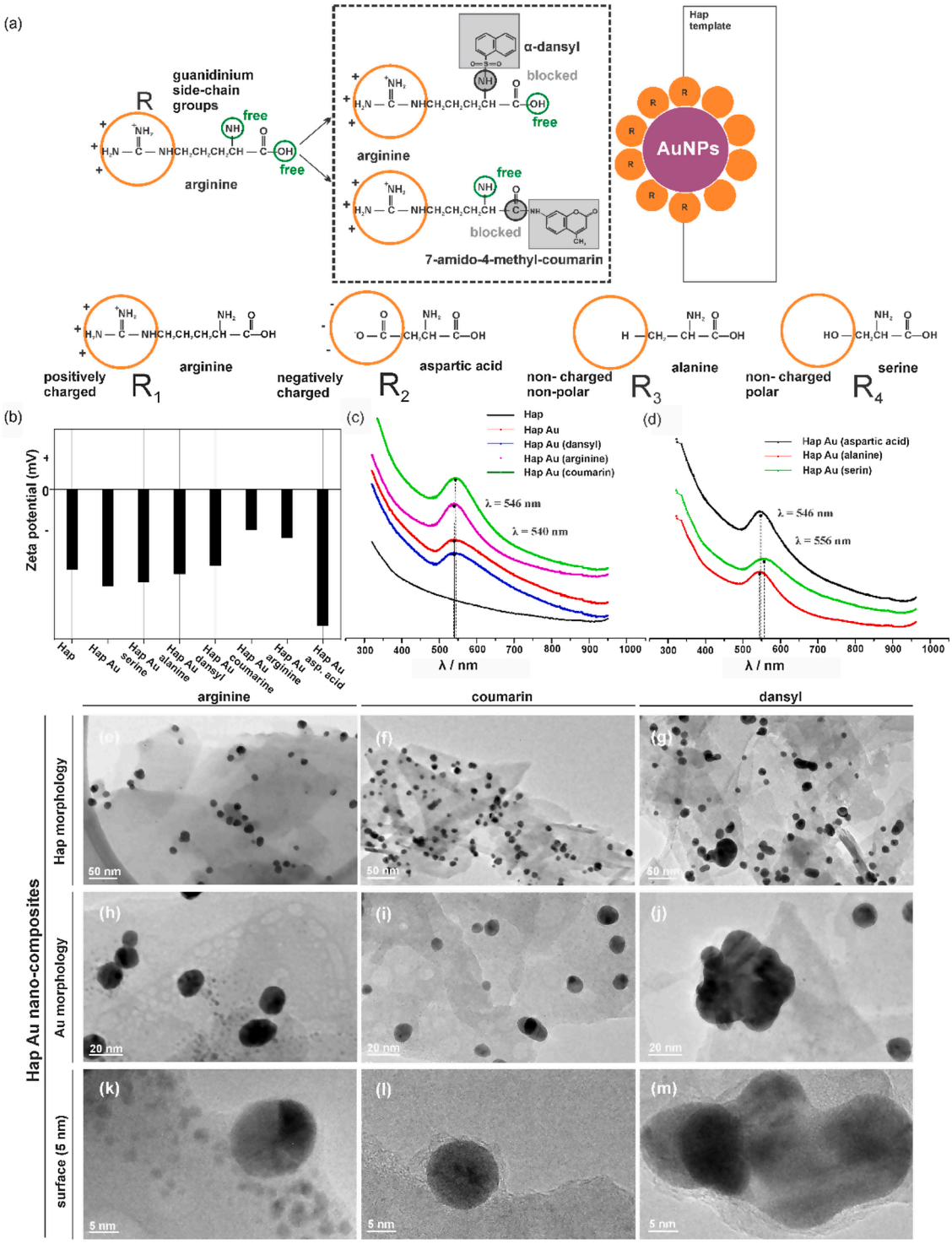

Fig. 1. Contact-based antimicrobials based on AuNPs: (a) functionalizing amino acids with selectively blocked main functional groups (amino and hydroxyl) and different combinations of polarity and charge (a), corresponding NP zeta potentials (b), UV–vis spectra (c,d) and TEM morphology and structure (e-m).

coumarin and dansyl-arginine have blocked COOH- and NH_2- groups, respectively. All of the particles were templated on the surface of apatite to design a system with external charge-driven antimicrobial activity without the ability to penetrate inside cells. If functionalization was performed using arginine (HAp Au arginine) or arginine with blocked COOH- groups (HAp Au coumarin), the negative charge of the apatite template (HAp) significantly decreased (Fig. 1b). This change did not occur when arginine with blocked NH_2- groups (HAp Au dansyl) was used (Fig. 1b). NH_2- groups have an essential role in the functionalization of nano-gold since they provide direct bonding between AuNPs and amino acids. Furthermore, for anionic aspartic acid (HAp Au aspartic acid) (also with free NH_2- and COOH- groups) as a functionalizing agent, the magnitude of the negative charge on the nano-gold increased (Fig. 1b).

The last confirmed that the α-amino group within the amino acid performs the bonding between the amino acid and the nano-gold, while side-chain groups (cationic guanidine groups in arginine and anionic carboxyl side-chain group in aspartic acid) remain free and available for interactions with surrounding components (i.e., bacterial and mammalian cells).

Depending on the availability of functional groups during the functionalization of nano-gold, the resulting optical properties varied, revealing differences in stability. In the case of nano-gold functionalized with arginine and arginine-coumarin (with free NH_2 groups), there is an intensive and narrow surface plasmon resonance (SPR) maximum, typical of uniform and well-stabilized nano-gold (Fig. 1c). The same occurs for NPs functionalized with anionic (aspartic acid) or non-charged (serine and alanine) amino acids (also with free NH_2) (Fig. 1d). However, for non-functionalized and arginine-dansyl-functionalized nano-gold (with blocked NH_2), the SPR maxima are quite broad, typical of non-stable structures. The latter was also confirmed during morphological study. AuNPs with arginine (Fig. 1e,h) and arginine-coumarin (Fig. 1f,i) functionalization are very stable, non-agglomerated and well distributed on the apatite surface. In both cases, single 15-nm AuNPs are coated with 2−3 nm of an amorphous layer (Fig. 1k,l). Arginine-coumarin enables better coverage of the apatite surface, a higher density of NPs per apatite template, and greater stability than arginine functionalization. In contrast, arginine-dansyl functionalization (with blocked NH_2) (Fig. 1g,j) provides larger, strongly agglomerated structures with significantly decreased stability (Fig. 1m). Free α- NH_2- groups are essential for providing effective functionalization and significantly contribute to the stability of the nanostructures, which are even more stable if the interactions of free COOH groups are blocked (as was observed in HAp/Au(coumarin)). FTIR of HAp Au nanoparticle functionalized with different amino acids, confirming their presence at their surface, are presented in Figure S1.

3.2. The nature of the amino acids affects the antimicrobial activity and cytotoxicity

Altering functional groups greatly affects the interactions of AuNPs with cells and contributes to their antimicrobial effects and cytotoxicity when they are in close contact. Testing the influence of functionalized AuNPs on the growth of different bacterial species revealed significant differences among arginine, arginine-coumarin (with blocked COOH-groups) and arginine-dansyl (with blocked NH_2- groups) (Fig. 2a summarizes reduction of bacterial colony unity (cfu/mL) and respective MIC values (Fig. 2b) for well-dispersed AuNPs in close contact with bacteria)). Although the functionalizing molecule was the same, blocking specific functional groups (coumarin-bonded COOH or dansyl-bonded NH_2-) altered their antimicrobial activity. More stable NPs functionalized with arginine-coumarin negatively affected and inhibited the growth of all three tested bacterial strains (Figure S2a,d,g). However, using the same functionalizing molecule (arginine) with blocked NH_2 groups within arginine-dansyl resulted in NPs that only slightly altered the kinetics of bacterial growth, and complete inhibition was not achieved (Figure S2b, e, h). The polarity and charge of functionalizing amino acids are also critical parameters, with determining roles in the ability of AuNPs to exert antimicrobial effects (Fig. 2b, Figure S3). Anionic aspartic acid-functionalized AuNPs only slightly inhibited bacterial growth and did not provide complete inhibition (Figure S3a). These findings are consistent with previous research showing a decrease in antimicrobial activity upon a change in surface charge orientation from cationic to anionic. [25,26] Serine, as a polar and non-charged amino acid at the AuNP surface, induced a similar change (Figure S3a). Otherwise, the activity was completely lost when non-polar and non-charged alanine was bound to the AuNP surface, with the resulting NPs barely affecting the growth of the investigated bacteria (Figure S3a). For all negative or non-charged amino acids used to functionalize the AuNPs, the Presto blue assay detected the metabolic

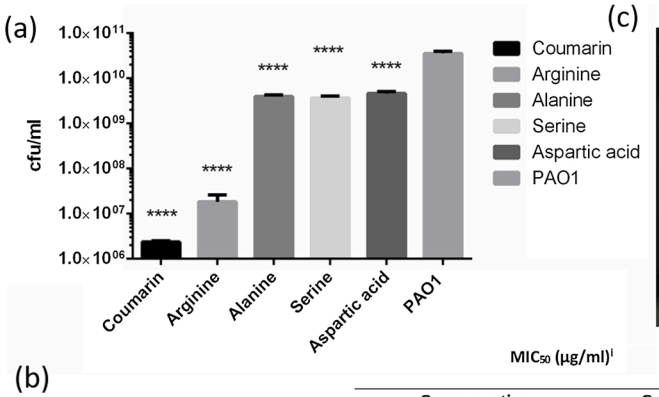

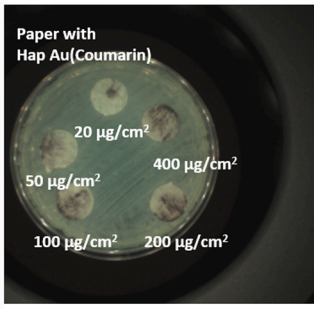

(b)

Functionalized AuNP[ii]	Polarity and charge[iii]	Gram-negative		Gram-positive	CC_{50}[iv] (μg/ml)
		E. coli	*P. aeruginosa*	*S. aureus*	
1. Arginine	Cationic, polar	400 (4.00)	400 (4.00)	500 (3.20)	1596±42
2. Coumarin	Cationic, polar	300 (5.44)	90 (18.13)	200 (8.16)	1632±111
3. Dansyl	Cationic, polar	>1000 (-)[e]	1000 (-)	350 (-)	(-)
4. Aspx. acid	Anionic, polar	600 (0.33)	600 (0.33)	600 (0.33)	198.0±14
5. Serine	Non-charged, polar	600 (-)	800 (-)	800 (-)	(-)
6. Alanine	Non-charged, non-polar	>1000 (-)	1000 (-)	>1000 (-)	(-)

Fig. 2. Antimicrobial activity and toxicity of contact- based antimicrobials: colony forming units (cfu) reduction obtained for PAO1 after close contact between bacteria and well-dispersed nanoparticles (a); minimal inhibitory concentration (MIC_{50}), cytotoxic concentrations (CC_{50}) and selectivity index (SI) values of so-dispersed nanoparticles (b), in absence of diffusion and contact with bacteria (nanoparticles deposited on paper discs) bacterial growth inhibition around discs in not obtained (c). Tested materials contained: 10 wt % (i) of AuNPs functionalized (ii) with 1- L-arginine, 2- L-arginine-7-amido-4-methylcoumarin (Coum.), 3- dansyl-L-arginine (Dansyl), 4- aspartic acid (Asp. acid), 5- serine and 6- alanine; polarity and charge of amino acids used for functionalization of AuNPs at pH = 7.4 (iii); MIC_{50} values for corresponding strains with SI calculated as CC_{50}/MIC_{50} (in parenthesis); CC_{50} measured in lung epithelial A549 cells (iv); (-) indicates that CC_{50} or SI was not determined due to low/absent antimicrobial activity); **** annotates significantly relevant differences ($p < 0.0001$) compare to PAO1 nanoparticle-free reference (One way ANOVA).

activity of the remaining viable cells in the three bacterial strains tested (Figure S3b). The contact is critically important for obtaining the antimicrobial activity and it was obtained only in case of well-dispersed AuNPs in direct contact with bacteria. After fixing NPs on top of the paper discs, due to an absence of diffusion there was no required contact with bacteria and activity is not obtained (absence of bacteria growth inhibition zones in Fig. 2c).

The nature of amino acids at the surface of AuNPs also affects their ability to interact with mammalian cells (as tested in human lung epithelial cells (A549), Fig. 2b and Figure S4). Similar to non-functionalized AuNPs, arginine-dansyl-functionalized AuNPs were inert and did not show a significant influence on cellular growth or morphology. However, the interactions of arginine and arginine-coumarin functionalizations with mammalian cells were more pronounced. Nevertheless, the concentrations of these NPs that enabled antimicrobial activity without affecting cellular viability were high and comparable to those reported in the references. On the other hand, changing from cationic to anionic AuNP surfaces (using aspartic acid) altered cellular toxicity (Fig. 2b). Consequently, we observed a significant decrease in CC_{50} and selectivity index (SI) for the anionic aspartic acid-functionalized AuNPs in comparison to the cationic arginine-functionalized NPs (Fig. 2b).

In summary, the stability of NPs and the charge at their surface were determining factors during their interactions with bacterial and lung epithelial cells. AuNPs with an anionic amino acid at the surface had stronger interactions with the cellular monolayers than with bacterial cells, showing higher affinity and greater damage to mammalian cells. In contrast, cationic AuNPs had a higher affinity to bacterial cells and

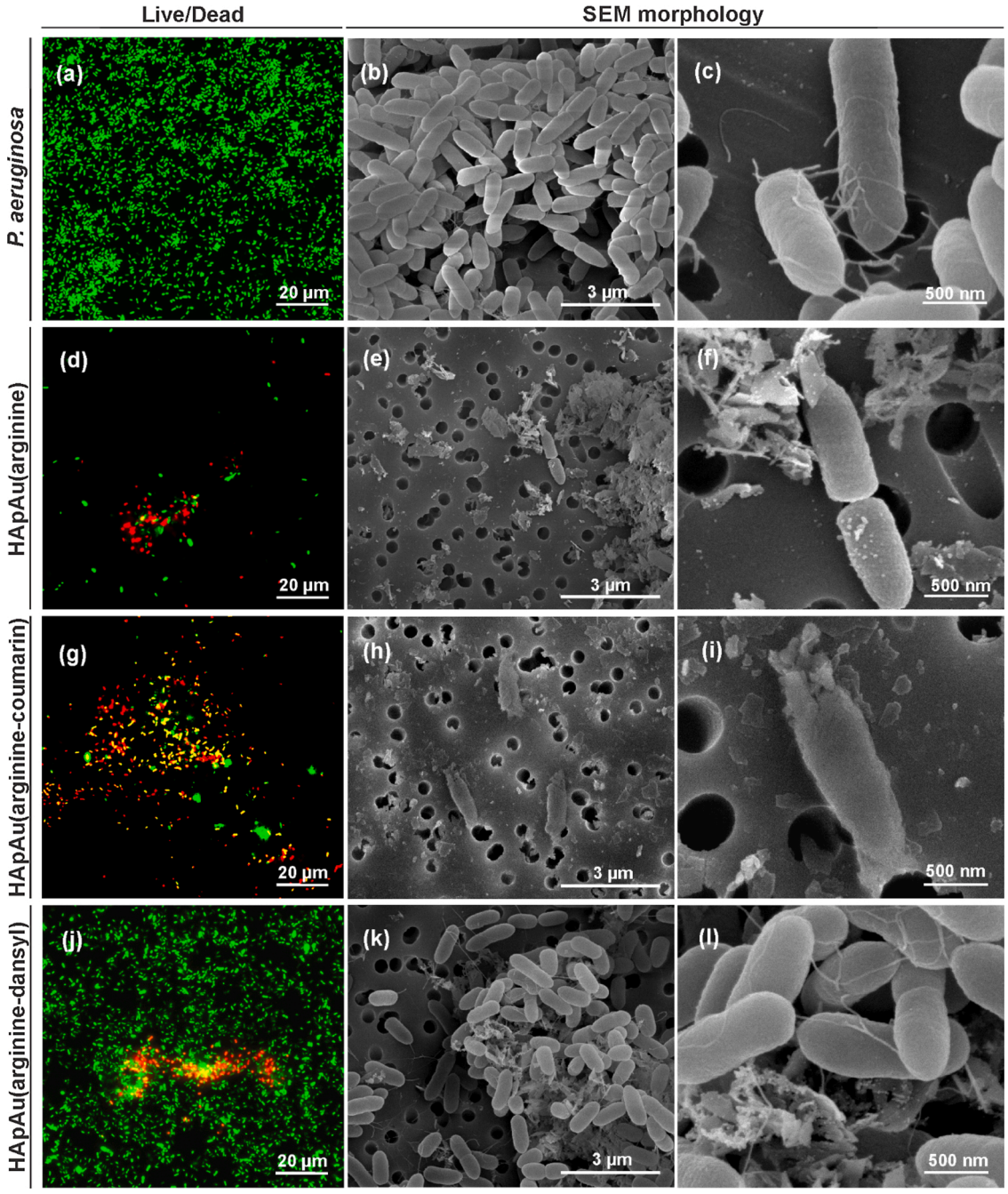

Fig. 3. Viability, morphological and structural properties of P. aeruginosa (a-c) after interactions with nano-gold/apatite functionalized with arginine (d-f), arginine-coumarin (g-i) and arginine-dansyl (j-l).

caused greater damage to them (Fig. 2b). Hence, the selectivity depends on the type of functionalization. The highest SI value (SI = 18) obtained for AuNPs functionalized with arginine-coumarin against *P. aeruginosa* highlights their prospects for further applications.

3.3. AuNP accumulation at the surface of bacterial membranes

NP accumulation, bacterial viability and morphology were studied in terms of available functional groups. Bacteria were exposed to AuNPs with free arginine, arginine-coumarin (with blocked COOH) and arginine-dansyl (with blocked NH_2).

In Live/Dead staining, *P. aeruginosa* treated with AuNPs (arginine-dansyl) was mainly viable (Fig. 3j) at similar levels to the reference (Fig. 3a). Morphologically, a high number of bacteria were mixed with Au(arginine-dansyl) NPs (Fig. 3k), but they were mainly smooth and lacked NPs visibly attached on their surface (Fig. 3l). Consequently, they retained the normal rod shape without detectable morphologic deformations. In contrast, treatment with the more stable arginine (Fig. 3d) and arginine-coumarin (Fig. 3g) AuNPs significantly reduced the number of observed bacteria, and most of them were dead. The bacteria were morphologically damaged (Fig. 3e,h) with altered bacterial cell walls and showed close contact between NPs and their surfaces (Fig. 3f,i).

The accumulation of NPs at the bacterial surface was finally confirmed using TEM (Fig. 4). Dark AuNPs were visible at the surface of the apatite template, as well as at the surface of bacteria in direct contact with the outer side of the bacterial membrane. Large apatite plates held AuNPs at their surface, providing contact with the outer surface of the bacterial wall and preventing their penetration inside bacterial cells. Bacteria exposed to arginine-dansyl AuNPs contained a very low fraction of NPs attached to bacteria (Fig. 4j,k), while in the case of arginine (Fig. 4d,e) and arginine-coumarin (Fig. 4g,h), bacteria were completely covered. Comparable results were obtained in gram-negative *E. coli* (Figure S5 and Figure S6).

In addition, in the case of *E. coli,* bacterial cell elongation was induced by AuNPs functionalized with arginine and arginine-coumarin, indicating the impairment of bacterial replication by these NPs (Figure S5d,g). Such a change in bacterial morphology is usually a consequence of their response to various types of stress (DNA damage or DNA replication inhibition) and can also be observed when using some antibiotics. [27] Most of the filamented bacteria were red stained, indicating damaged membranes or dead cells. Similar to *P. aeruginosa*, morphological analysis of the *E. coli* cell wall revealed significant cell damage (Figure S5), while structural investigations confirmed the accumulation of AuNPs at the bacterial surface (Figure S6). NPs were found in very close contact with the outer side of the bacterial wall, which enabled the required interactions to promote membrane disintegration (Figure S6).

In gram-positive *S. aureus*, AuNPs with arginine-dansyl (Fig. 5) induced a decrease in bacterial cell numbers, which was an interesting

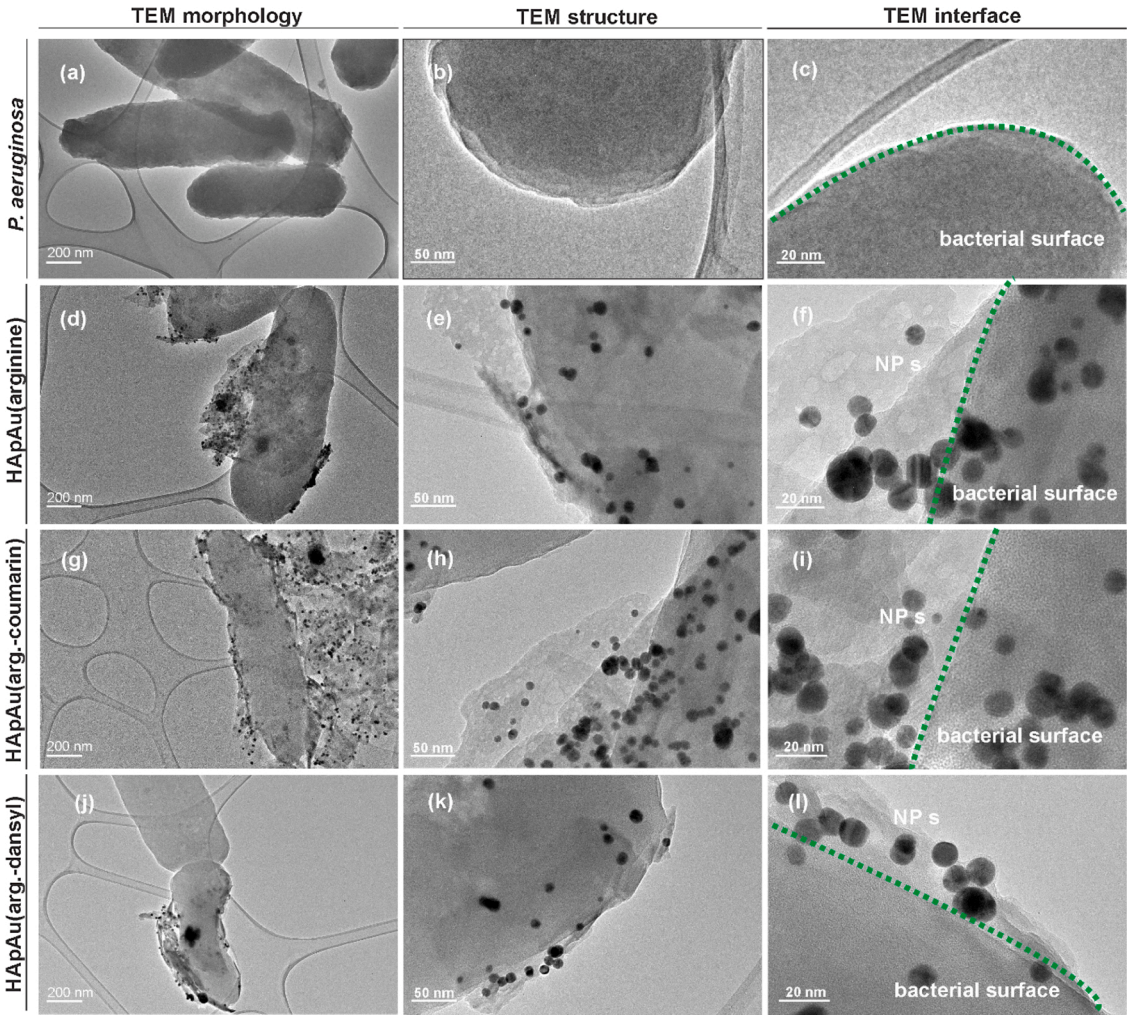

Fig. 4. Morphology, structure and bacteria-NP interface for *P. aeruginosa* (a-c) after interaction with nano-gold/apatite functionalized with arginine (d-f), arginine-coumarin (g-i) and arginine-dansyl (j-l).

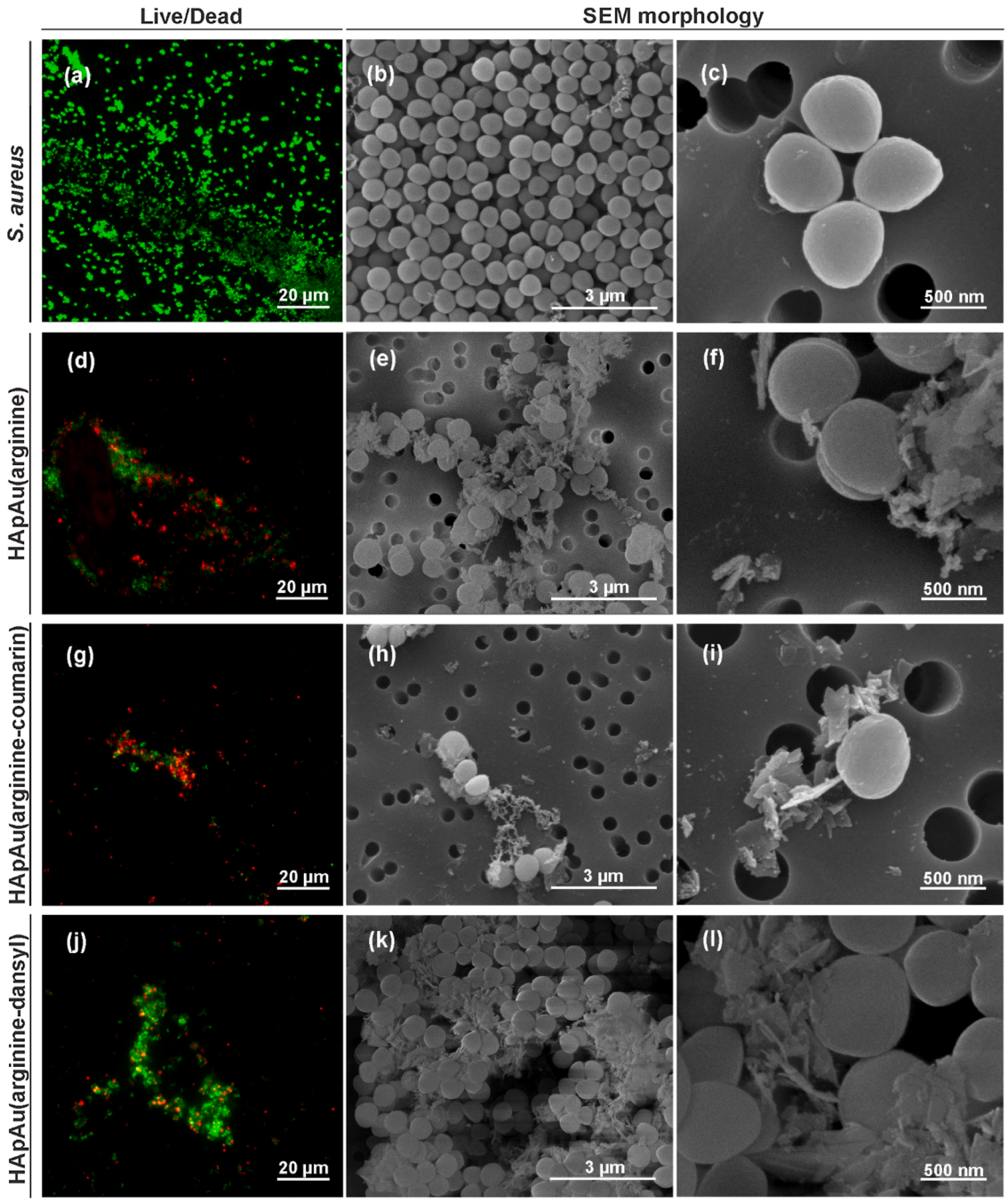

Fig. 5. Viability and morphological and structural properties *of S. aureus* (a-c) after interactions with nano-gold/apatite functionalized with arginine (d-f), arginine-coumarin (g-i) and arginine-dansyl (i-l).

difference from the effect in gram-negative bacteria. SEM analysis confirmed a reduction in bacterial cells from arginine-dansyl (Fig. 5k) to arginine (Fig. 5e) to arginine-coumarin (Fig. 5h). *S. aureus* bacteria retained their usual shape and size, without microscopically visible deformations of the cell wall and with higher viability for the dansyl NPs (Fig. 5j). Increased cell debris was observed in the SEM images (Fig. 5e, h, k) compared to the untreated sample (Fig. 5b). However, the debris was not clearly distinguishable from NPs. Further observations performed by TEM of the interface between AuNPs and the outer side of the bacterial cell wall revealed an intense accumulation of AuNPs, which was shared among the three types of functionalizing molecules (arginine, arginine-coumarin, and arginine-dansyl) (Fig. 6). There was also a massive density of NPs found in direct contact with *S. aureus*, which resulted in nanoscale shrinkage and deformations of the bacterial wall, which may contribute to the observed antimicrobial activity (Fig. 2b).

A previous study showed decreased potency of functionalized AuNPs against gram-positive bacteria. This was explained by the lower ability of NPs to penetrate the multilayered peptidoglycan envelope of gram-positive bacteria [26]. However, it seems that their interactions with the membrane in gram-positive bacteria and limited ability to provide massive cell disintegration (as observed for templated AuNPs without the ability to cross the bacterial wall) is another relevant factor.

3.4. Charge of amino acid-functionalized nano-gold enables the selective disruption of bacterial versus mammalian membranes

The membrane structure in gram-positive and gram-negative bacteria treated with functionalized AuNPs was further investigated using

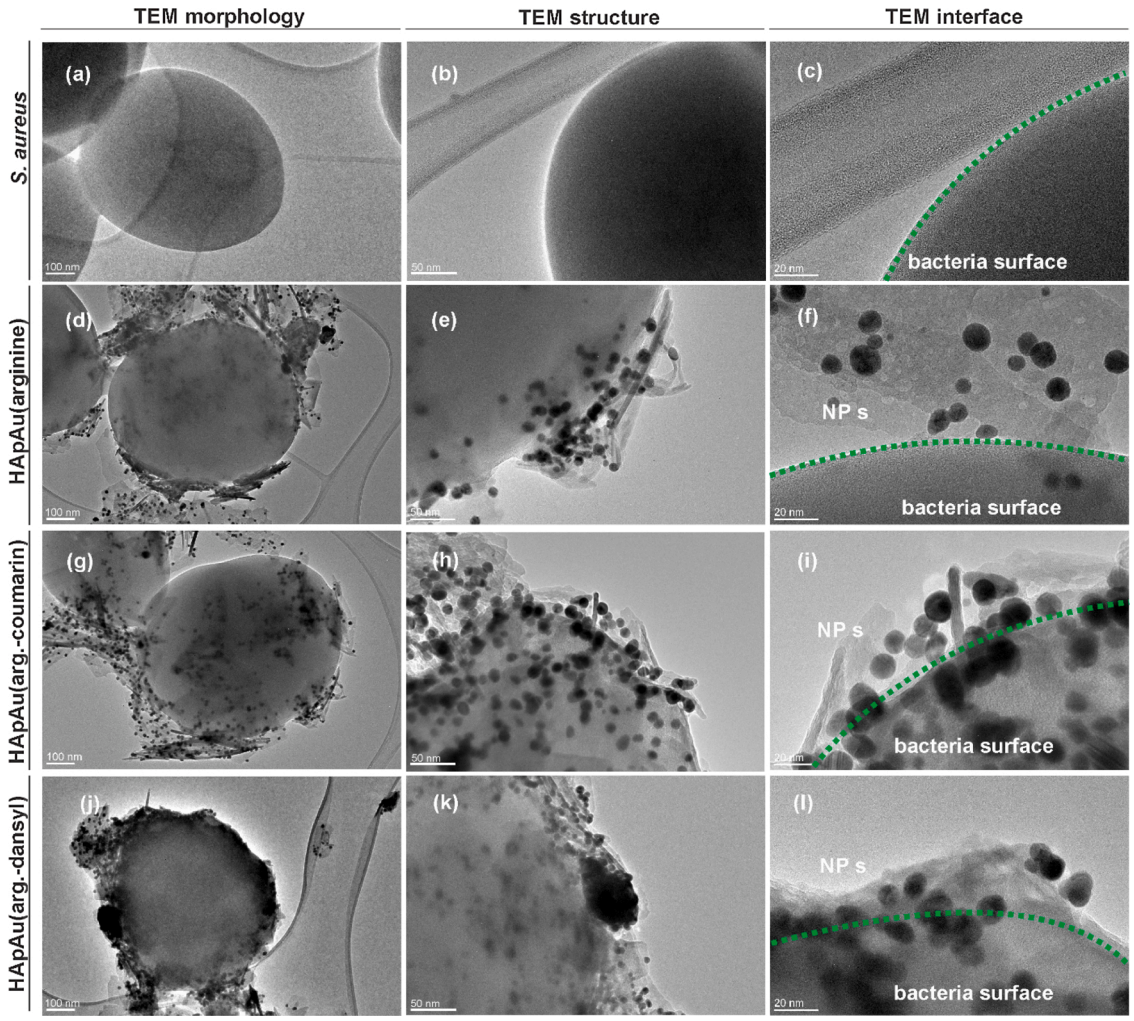

Fig. 6. Morphology, structure and bacteria-NPs interphase for S. aureus (a-c) after interaction with nano-gold/apatite functionalized with arginine (d-f), arginine-coumarin (g-i) and arginine-dansyl (j-l).

co-staining with FM 4-64 (red) and DAPI (blue). Lipophilic FM 4-64 is membrane specific and preferentially stains the outer leaflet of the bacterial membrane [28], while DAPI specifically binds to DNA. In combination, they are capable of detecting changes in membrane permeability and morphological changes [29].

Co-staining was applied for bacteria exposed to AuNPs functionalized with cationic arginine and anionic aspartic acid. In *P. aeruginosa,* reference staining clearly enabled the visualization of FM 4-64 red-stained intact membrane morphology and blue-stained DNA inside cells (Figure 7a_1). Very similar morphology of the intact membrane and the DNA inside cells was observed after staining bacterial cells previously exposed to anionic, aspartic acid-functionalized AuNPs (Figure 7a_2). For cationic arginine functionalization of the AuNPs, the staining revealed damage and discontinued the *P. aeruginosa* membrane, with increased permeability indicated by localized accumulations of red stain in the inner side of the membrane, as well as in the cytosol (Figure 7a_3). DAPI staining delocalized outside the cell, possibly due to leakage of the intracellular DNA content. Similar changes in membrane morphology and permeability were also observed in *E. coli* (Figure S7).

Modifications to the membrane permeability detected in the gram-negative bacteria were in line with SEM and TEM investigations (Fig. 3, Fig. 4, Figure S5, Figure S6), and they were expected considering the detected damage to the morphology and structure of *E. coli* and *P. aeruginosa* cells. However, for gram-positive *S. aureus*, in addition to shrinking and deformed cell structure, SEM and TEM did not provide clear evidence of membrane damage (Fig. 5, Fig. 6). For cells affected by cationic functionalization, a high content of FM 4-64 was found to accumulate in the cytosol, with a DNA content detected outside of the cells (Figure 7a_6). Therefore, FM 4-64 /DAPI co-staining of *S. aureus* treated with cationic arginine-AuNPs undoubtedly confirmed an increased membrane permeability, observed as a non-homogeneous thickening of the inner side of the membrane (Figure 7a_6).

In addition to their influence on bacterial cell walls, we investigated how functionalized AuNPs interact with mammalian cell membranes and consequent changes they promote on their morphology. Morphologic characteristics of A549 lung epithelial cells were observed after co-staining the cellular monolayer with ethidium homodimer III (EthD III)/ DAPI/wheat germ agglutinin (WGA). WGA has a high affinity to bind N-acetyl-D-glucosamine residues [30], especially those located at the surface of intestinal and alveolar epithelial cells [31], and it is therefore suitable for labelling lung cell membranes. DAPI (blue) and EthD III (red) are both specific for DNA staining inside the cell. While DAPI is membrane permeable, EthD III is impermeable for viable cells (with intact and non-damaged membranes) and can selectively bind the DNA of dead or dying cells [32]. In combination, they are suitable for determining cellular viability.

A549 cells treated with AuNPs functionalized with cationic arginine and arginine-coumarin amino acids (Fig. 7b_2) were characterized by similar morphology to that observed in control cells (Figure 6b_1). As indicated in Fig. 7, NPs were present in particular areas as aggregates

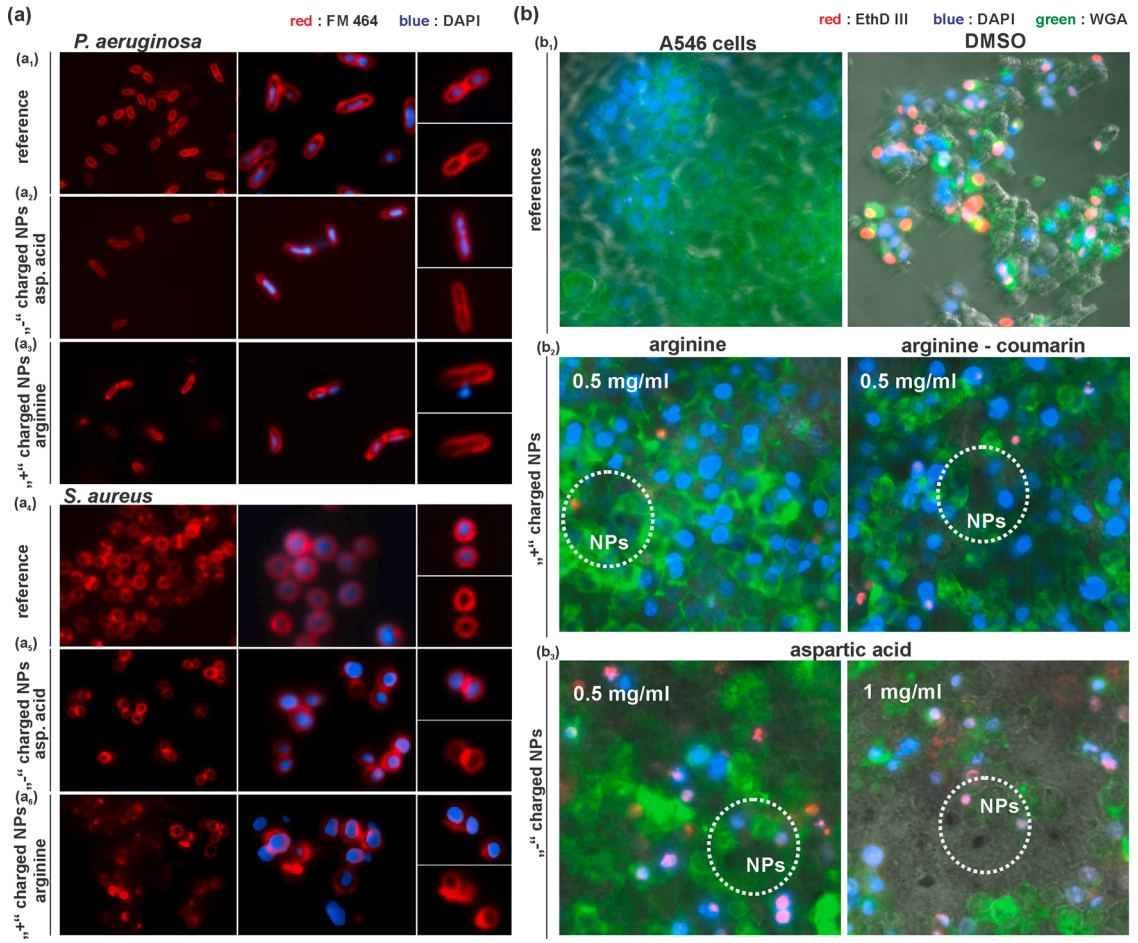

Fig. 7. NP interactions with membranes: (a) compactness of bacterial membranes in a gram-negative strain (*P. aeruginosa*) and a gram-positive strain (*S. aureus*) before (a_1,a_4) and after treatment with NPs functionalized with negatively (a_2,a_4) and positively (a_3,a_6) charged amino acids (FM 4-64 and DAPI); (b) morphological characteristics of human A549 lung epithelial cells: cell reference and cells affected by DMSO (b_1); cells with positively charged nano-gold functionalized with arginine-coumarin and arginine-dansyl (b_2); cells with negatively charged nano-gold functionalized with aspartic acid (b_3) (EthD III/DAPI/WGA); "NPs" labelling refers to observed NP aggregates.

that were in direct contact with A549 cells, without causing cellular detachment or decreasing their confluence. A low fraction of cells were red stained, indicating dying cells with a disrupted membrane. In the case of AuNPs functionalized with anionic aspartic acid, even at lower concentrations of NPs, an increased fraction of cells were red stained, indicating a disrupted membrane. Otherwise, higher concentrations induced disintegration of the cellular monolayer and provided a noticeable decrease in cell density with a significant increase in red-stained cells (Figure 7b_3) and similar DMSO-treated cells (Figure 7b_2).

In summary, the results confirm that AuNPs functionalized with anionic amino acids are prone to have more intensive interactions with mammalian cells than AuNPs functionalized with cationic amino acids, contributing to their toxicity and cellular membrane damage.

3.5. *Enzymatic digestion of functionalized AuNPs and antimicrobial activity of post-digested contact-based antimicrobials*

As mentioned above, the most critical property of contact-based antimicrobials (AMPs and some polymers) that significantly influences their potency, half-life, and stability is their ability to resist enzymatic digestion. One of the predicted advantages of amino acid-functionalized AuNPs in designing contact-based antimicrobials was their resistance to enzymatic degradation due to the absence of peptide bonds that could be enzymatically hydrolysed by proteases. To show this benefit of functionalized AuNPs as well as to exclude the possibility that antimicrobial properties of amino acid AuNPs originate from peptides formed on their surface, we exposed them to two different serine proteases, trypsin and protease K, which are frequently used to test the sensitivity of AMPs and polymers to enzymatic digestion. [33–35]

While proteinase K is characterized by a very broad spectrum and non-specificity, trypsin favours the cleavage of peptide chains at peptide bonds formed by arginine and lysine, which makes it more selective. As amino acid-functionalized AuNPs are deposited on apatite, which consists of calcium phosphate, the composite slowly releases Ca^{2+} ions. Because the stability and activity of proteinase K are improved in the presence of Ca^{2+} ions, [36] it was a highly relevant enzyme model for testing enzymatic degradation. On the other hand, as the trypsin cleavage site is exclusively related to arginine residues [37], this enzyme is highly useful for determining the degradability of cationic AuNPs functionalized with this amino acid.

The protease activity of both enzymes was tested using bovine serum albumin (BSA) as a reference (Fig. 8). After enzymatic digestion of the different AuNPs together with BSA, protein degradation was determined using SDS-PAGE. The results showed that trypsin partially degraded BSA, while proteinase K completely degraded BSA, confirming the activity of both enzymes (Fig. 8a). After exposure to enzymes, the AuNPs were washed and re-tested for antimicrobial activity. The metabolic activity of bacteria exposed to different AuNP concentrations was tested for three groups of AuNPs treated with trypsin, AuNPs treated with proteinase K and reference (non-treated) AuNPs. In all three cases, the

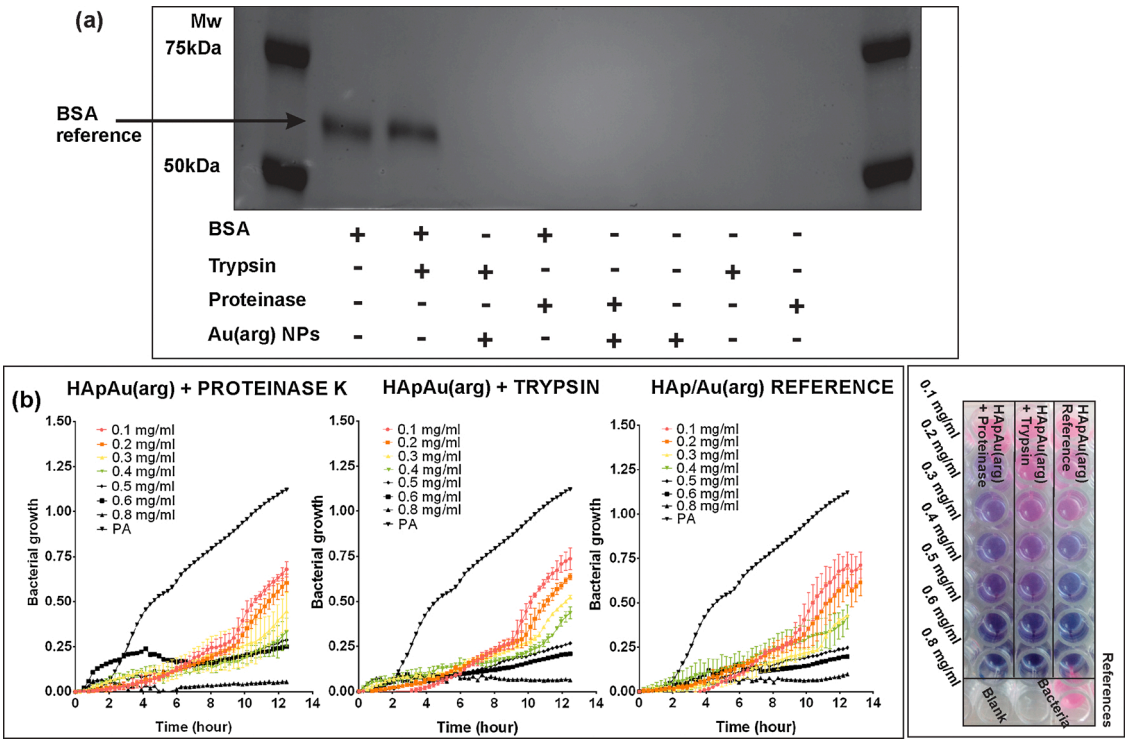

Fig. 8. Enzymatic digestion of arginine-functionalized nano-Au/apatite and post-digestion antimicrobial activity in *P. aeruginosa*: (a) activity of trypsin and proteinase K in NPs in comparison to degradation of BSA protein used as a reference; (b) metabolic activity of *P. aeruginosa* after exposure to increasing contents of NPs before and after digestion with trypsin and proteinase K; (c) kinetics of bacterial growth in the presence of NPs digested with enzymes and non-digested NPs used as a reference.

Presto blue test showed a complete absence of metabolic activity at concentrations reaching to the MIC_{100} value of AuNPs functionalized with arginine. The same was also observed during the investigation of the kinetics of bacterial growth in the presence of these three series of NPs with increasing concentrations (Fig. 8c). Bacteria were grown in the same manner regardless of the enzyme treatment. Consequently, we confirmed the resistance of arginine-functionalized AuNPs to the hydrolytic activity of proteases as an essential characteristic of these contact-based antimicrobials.

In summary, this investigation illustrates the mechanism and clearly explains the phenomena taking place at the interface between amino acid-functionalized AuNPs and bacterial surfaces. The stability of the formed structures to enzymatic degradation is attributed to their configuration. Instead of polypeptide formation, they are designed using direct bonding between the AuNPs and the amino acids, without the formation of cleavable functional groups (such as peptide bonds), which we believe is an additional factor in their enzymatic resistance. The concept presented here for designing contact-based antimicrobials confirms that with proper selection of functionalizing molecules (characterized by polarity and positively charged groups, freely available for subsequent interactions), stability can be combined with optimal selectivity for interactions between bacterial and mammalian cells. This concept is tailorable to design a range of other similar structures for charge-driven selectivity in combination with good enzymatic stability. As self-antimicrobial, antibiotic-free NPs, these structures offer interesting concepts for the further design of stable contact-based antimicrobials and the further exploration of their capacities to combat AMR strains.

4. Conclusions

Designing contact-based antimicrobials using amino acid-functionalized AuNPs is a highly feasible way to avoid some of the most critical problems associated with this class of antimicrobials, including sensitivity to extreme chemical conditions, enzymatic deactivation, low bioavailability and very high production costs. The stability, polarity, and charge of amino acids used in designing the surface of AuNP nanostructures have a crucial role in developing their performance. Direct bonding between polar, cationic amino acids and AuNPs is a way to eliminate cleavable bonds and thereby ensure drastic improvement in enzymatic sensitivity. The approach could be applied as a useful guideline for designing the next generation of self-antimicrobial, antibiotic-free NPs that are particularly stable in the presence of enzymes. We believe that the described approach presents a novel way to explore contact-based antimicrobials as a prospective class of antimicrobials applicable against AMR bacteria.

Funding

This work has been funded by the European Commission under Horizon 2020's Marie Skłodowska-Curie Actions COFUND scheme (Grant 712754) and by the Severo Ochoa programme of the Spanish Ministry of Science and Competitiveness (Grant SEV-2014-0425 (2015-2019)). ET was supported by grants from the Spanish Ministerio de Economia y Competitividad (MINECO/FEDER) (BIO2015-63557-R), Generalitat de Catalunya (2014 SGR01260 and CERCA programme), the Catalan and Spanish Cystic Fibrosis foundations and La Caixa Foundation. Additional funding support has been provided to MV by grants from the Slovenian Research Agency (ARRS) (Grants J2-8169 and N2-0150).

CRediT authorship contribution statement

Marija Vukomanovic: Conceptualization, Investigation, Writing - original draft, Funding acquisition, Visualization. **Maria del Mar Cendra:** Investigation, Writing - review & editing, Visualization. **Aida Baelo:** Investigation, Writing - review & editing, Visualization. **Eduard Torrents:** Conceptualization, Writing - review & editing, Funding

acquisition, Supervision.

Declaration of Competing Interest

The authors report no declarations of interest.

Acknowledgements

The authors are grateful to Angel Blanco Blanes and Dr Samuel Sanchez from the Smart Nano-Bio-Devices group at IBEC for zeta potential measurements as well as to Damjan Vengust from the Advanced Materials Department, JSI, for TEM analyses.

Appendix A. Supplementary data

Supplementary material related to this article can be found, in the online version, at doi:https://doi.org/10.1016/j.colsurfb.2021.112083.

References

[1] L.S. Tavares, C.S.F. Silva, V.C. de Souza, V.L. da Silva, C.G. Diniz, M.O. Santos, Front. Microbiol. 4 (2013) 412.
[2] M.N. Gwynn, A. Portnoy, S.F. Rittenhouse, D.J. Payne, Ann. N. Y. Acad. Sci. 1213 (2010) 5–19.
[3] S.B. Singh, K. Young, L.L. Silver, Biochem. Pharmacol. 133 (2017) 63–73.
[4] E.D. Brown, G.D. Wright, Nature 529 (2016) 336–343.
[5] R. Tommasi, D.G. Brown, G.K. Walkup, J.I. Manchester, A.A. Miller, Nat. Rev. Drug Discov. 14 (2015) 529–542.
[6] N. Beyth, Y. Houri-Haddad, A. Domb, W. Khan, R. Hazan, Evid. Based Complement. Alternat. Med. (2015), 246012.
[7] C. Adlhart, J. Verran, N.F. Azevedo, H. Olmez, M.M. Keinänen-Toivola, I. Gouveia, L.F. Melo, F. Crijns, J. Hosp. Infect. 99 (3) (2018) 239–249.
[8] K. Peng, T. Zou, W. Ding, R. Wang, J. Guo, J.J. Round, T. Weiping, L. Chao, H. Jianqing, RSC Adv. 7 (2017) 24903–24913.
[9] K. Kuroda, G.A. Caputo, Wiley Interdiscip. Rev. Nanomed. Nanobiotechnol. 5 (1) (2013) 49–66.
[10] P. Kurt, L. Wood, D.E. Ohman, K.J. Wynne, Langmuir 23 (2007) 4719–4723.
[11] M. Vukomanović, V. Žunič, S. Kunej, B. Jančar, S. Jeverica, R. Podlipec, D. Suvorov, Sci. Rep. 7 (2017) 4324–4337.
[12] B. Casciaro, F. Cappiello, M. Cacciafesta, M.L. Mangoni, Front. Chem. 25 (2017) 26.
[13] P. Wadhwani, N. Heidenreich, B. Podeyn, J. Bürck, A.S. Ulrich, Biomater. Sci. 28 (2017) 817–827.
[14] H.K. Daima, P.R. Selvakannan, R. Shukla, S.K. Bhargava, V. Bansal, PLoS One 8 (10) (2013), e79676.
[15] C. Tao, Lett. Appl. Microbiol. 67 (6) (2018) 537–543.
[16] M. Vukomanovic, in: A. Ficai, A.M. Grumezescu (Eds.), Advanced Nanocomposites With Noble Metal Antimicrobial Nanoparticles: How to Design a Balance Among Antimicrobial Activity, Bioactivity, and Safe Delivery to the Place of Infection in Nanostructures for Antimicrobial Therapy: Nanostructures in Therapeutic Medicine Series, Vol. 28, Elsevier, Amsterdam, the Netherlands, 2017.
[17] N.S. Parachin, O.L. Franco, Front. Microbiol. 5 (2014) 147.
[18] L.T. Nguyen, E.F. Haney, H.J. Vogel, Trends Biotechnol. 29 (2011) 464–472.
[19] R.E.W. Hancock, E.F. Haney, E.E. Gill, Nat. Rev. Immunol. 16 (2016) 321–334.
[20] M. Vukomanovic, S. Skapin, D. Suvorov, WO2013187846A1, 2015.
[21] M. Vukomanović, M. Logar, S. Škapin, D. Suvorov, J. Mater. Chem. B 2 (2014) 1557–1564.
[22] C.A. Fitch, G. Platzer, M. Okon, B.E. Garcia-Moreno, L.P. McIntosh, Protein Sci. 24 (5) (2015) 752–761.
[23] M. Jevtić, M. Mitrić, S. Škapin, B. Jančar, N. Ignjatović, D. Uskoković, Cryst. Growth Des. 8 (7) (2008) 2217–2222.
[24] M. Vukomanovic, E. Torrents, J. Nanobiotechnology 17 (2019) 21–32.
[25] X. Li, S.M. Robinson, A. Gupta, K. Saha, Z. Jiang, D. F.Moyano, A. Sahar, M. A. Riley, V.M. Rotello, ACS Nano 8 (2014) 10682–10686.
[26] S. Huo, Y. Jiang, A. Gupta, Z. Jiang, R.F. Landis, S. Hou, X.J. Liang, V.M. Rotello, ACS Nano 10 (2016) 8732–8737.
[27] S.S. Justice, D.A. Hunstad, L. Cegelski, S.J. Hultgren, Nat. Rev. Microbiol. 6 (2008) 162–168.
[28] S. Lewenza, D. Vidal-Ingigliardi, A.P. Pugsley, J. Bacteriol. 188 (2006) 3516–3524.
[29] P. Nonejuie, M. Burkart, K. Pogliano, J. Pogliano, Proc. Natl. Acad. Sci. 110 (2013) 16169–16174.
[30] M. Monsigny, A.C. Roche, C. Sene, R. Maget-Dana, F. Delmotte, Eur. J. Biochem. 104 (1980) 147–153.
[31] C.M. Lehr, J. Control. Release 65 (2000) 19–29.
[32] J.M. Laing, M.D. Gober, E.K. Golembewski, S.M. Thompson, K.A. Gyure, P. J. Yarowsky, L. Aurelian, Mol. Ther. 13 (5) (2006) 870–881.
[33] N. Papo, Z. Oren, U. Pag, H.G. Sahl, Y. Shai, J. Biol. Chem. 277 (37) (2002) 33913–33921.
[34] B.J. Moncla, K. Pryke, L.C. Rohan, P.W. Graebing, Adv. Biosci. Biotechnol. 2 (6) (2011) 404–408.
[35] Y.P. Shin, H.J. Park, S.H. Shin, Y.S. Lee, S. Park, S. Jo, Y.H. Lee, I.H. Lee, Antimicrob. Agents Chemother. 54 (7) (2010) 2855–2866.
[36] J. Bajorath, W. Hinrichs, W. Saenger, Eur. J. Biochem. 176 (2) (1988) 441–447.
[37] J.V. Olsen, S.E. Ong, M. Mann, Mol. Cell. Proteomics 3 (6) (2004) 608–614.